International Journal of Applied Earth Observation and Geoinformation 23 (2013) 397–410

Contents lists available at SciVerse ScienceDirect

International Journal of Applied Earth Observation and Geoinformation

journal homepage: www.elsevier.com/locate/jag

Establishing and assessing the Integrated Surface Drought Index (ISDI) for agricultural drought monitoring in mid-eastern China

Jianjun Wu[a], Lei Zhou[b,*], Ming Liu[a], Jie Zhang[c], Song Leng[a], Chunyuan Diao[d]

[a] Academy of Disaster Reduction and Emergency Management, MOCA/MOE, Beijing Normal University, Beijing 100875, China
[b] China National Environmental Monitoring Center, Beijing 100012, China
[c] Department of Geography, University of Maryland, College Park, MD 20742, United States
[d] Department of Geography, University at Buffalo, The State University of New York, Buffalo, NY 14261, United States

ARTICLE INFO

Article history:
Received 14 August 2012
Accepted 22 November 2012

Keywords:
Drought
Drought indices
Data mining
ISDI

ABSTRACT

Accurately monitoring the temporal, spatial distribution and severity of agricultural drought is an effective means to reduce the farmers' losses. Based on the concept of the new drought index called VegDRI, this paper established a new method, named the Integrated Surface Drought Index (ISDI). In this method, the Palmer Drought Severity Index (PDSI) was selected as the dependent variable; for the independent variables, 12 different combinations of 14 factors were examined, including the traditional climate-based drought indicators, satellite-derived vegetation indices, and other biophysical variables. The final model was established by fully describing drought properties with the smaller average error (relative error) and larger correlation coefficients. The ISDI can be used not only to monitor the main drought features, including precipitation anomalies and vegetation growth conditions but also to indicate the earth surface thermal and water content properties by incorporating temperature information. Then, the ISDI was used for drought monitoring from 2000 to 2009 in mid-eastern China. The results for 2006 (a typical dry year) demonstrate the effectiveness and capability of the ISDI for monitoring drought on both the large and the local scales. Additionally, the multiyear ISDI monitoring results were compared with the actual drought intensity using the agro-meteorological disaster data recorded at the agro-meteorological sites. The investigation results indicated that the ISDI confers advantages in the accuracy and spatial resolution for monitoring drought and has significant potential for drought identification in China.

1. Introduction

Drought is an important disaster, and its impacts on agriculture are enormous. The drought events also have huge harm to economies, societies and environments (Wilhite, 2002). In recent decades, the impacts of drought have escalated in response to population increase, environmental degradation, industry development, and fragmented government authority in water and natural resources management (Wilhite, 2002). China is a region that is prone to natural disasters. The grain loss caused by drought accounted for 60% of all grain losses caused by meteorological disasters, resulting in 58% or more of economic losses (Li et al., 1999). The frequent occurrence of drought, coupled with the impact of global warming, poses an increasingly severe threat to the Chinese agricultural production (Ma et al., 2004).

Drought differs from other natural disasters, such as floods, typhoons, and earthquakes (Wilhite, 2000). First, the effects of drought often accumulate slowly over a considerable period of time and may linger for years after the termination of the event, and both the onset and end of drought are difficult to determine (Tannehill, 1947). Second, the absence of a precise and universally accepted definition of drought adds to the confusion regarding drought research and identification (Dracup et al., 1980; Gibbs, 1975; Wilhite et al., 1987; Wilhite and Glantz, 1985). Agricultural drought refers to a period with declining soil moisture content and consequent crop failure (Son et al., 2012; Boken et al., 2005). Considering the temporal and spatial complexity of a drought, it is difficult to accurately and quantitatively identify the onset, end, and duration of drought. During the latter part of 20th century, scientists established various drought indices based on different discipline perspectives and their own understanding of the definition of drought. The drought monitoring indices based on traditional meteorological data were developed first (Wilhite and Glantz, 1985). The meteorological indices offer advantages in quantitatively characterizing drought and applicability in different regions. The Standardized Precipitation Index (SPI) based on simple principles has been widely used all over the world, which allows for monitoring and assessment of drought at different timescales, and shows good comparability between different areas (Guttman, 1999; McKee et al., 1993). The Palmer Drought Severity Index

* Corresponding author. Tel.: +86 10 84943253; fax: +86 10 84949045.
E-mail address: zhoulei8341@163.com (L. Zhou).

0303-2434/$ – see front matter © 2012 Elsevier B.V. All rights reserved.
http://dx.doi.org/10.1016/j.jag.2012.11.003

(PDSI) is established based on a simplified water balance principle. It takes into account the antecedent precipitation and water supply and demand, involving calculations related to evapotranspiration, soil water supply, runoff, and surface soil water loss (Palmer, 1965; Alley, 1984; Guttman, 1997). The PDSI is suitable not only for monthly drought monitoring but also for weekly drought detection (Bayarjargal et al., 2006; Dai and Trenberth, 1998; WMO, 1975).

Remote sensing technology makes it possible for retrieval of soil moisture, and vegetation conditions across large areas. The Moderate Resolution Imaging Spectroradiometer (MODIS) data plays an increasingly important role in drought monitoring and assessment (Wan et al., 2004), owing to the associated rich spectral information, short revisit cycle, and convenient data access means. The Normalized Difference Vegetation Index (NDVI) is the most widely used indicator of vegetation growth conditions and vegetation coverage, which has been successfully used to estimate vegetation biomass and assess environmental conditions (Chen et al., 2012; Bannari et al., 1995; Justice et al., 1985; Rasmussen, 1998; Tucker and Sellers, 1986); this is why NDVI is widely used in agricultural drought monitoring (Gutman, 1990; Henricksen and Durkin, 1986; Tucker, 1989; Tucker and Choudhury, 1987). Vegetation Condition Index (VCI) is developed based on NDVI time-series data (Kogan, 1990). Compared to NDVI, VCI can better reflect the relationships between the vegetation growth conditions and the precipitation and can minimize the interference of other environmental factors when used to monitor regional agricultural drought during the growth season (Liu and Kogan, 1996; Wang et al., 2001a,b). Percent of Average Seasonal Greenness (PASG) is another index based on historical remote sensing vegetation index sequence (Brown et al., 2008). PASG evaluates vegetation growth conditions by calculating the percentage between the greenness in specific period and the average historical greenness over the same period (Tadesse et al., 2005).

Surface temperature is also an indicator of drought. Drought induces water deficit, which would reduce transpiration and lead to the rise of surface temperature, while relative low temperature stands for the normal healthy status of vegetation under the same condition of vegetation coverage (Jackson et al., 1981; Wan and Dozier, 1996). The Temperature Condition Index (TCI) is developed based on the principle mentioned above and has been widely used in drought monitoring (Kogan, 1995). Vegetation growth conditions will be affected by drought. There will be a decrease in the vegetation index, such as NDVI, and an increase in the canopy temperature because of the stomata closure to minimize water loss by transpiration (McVicar and Jupp, 1998). Thus, the slope of Ts (Surface Temperature)/NDVI can be used to assess the vegetation drought level. The application of the Ts-NDVI method in drought monitoring has been investigated by many researchers (Berliner et al., 1984; Mottram et al., 1983; Pinter et al., 1979). The Vegetation Supply Water Index (VSWI) has been developed based on the theory mentioned above (Bayarjargal et al., 2006; Gillies and Carlson, 1995; Gillies et al., 1997; Price, 1990). Using the Ts/NDVI method, McVicar (2001) rapidly assessed the 1997 drought in Papua New Guinea and validated the effectiveness of this method in drought monitoring (McVicar and Bierwirth, 2001).

Drought is a complex natural disaster. However, each drought index has its own advantages and weaknesses in drought monitoring. Almost all the drought indices are based on specific geographical and temporal scales; it is difficult to spread its applicability all over the world. Because of the meteorological drought indices using discrete, point-based meteorological measurements collected at weather station locations, the results have restricted level of spatial precision for monitoring drought patterns. Remote sensing technology provides alternative data for operational drought monitoring, with advanced temporal and spatial characteristics (Misshra and Singh, 2010). However, additional information still needs to be incorporated so as to thoroughly explain the anomaly in vegetation caused by drought. Besides, to achieve a more accurate description of drought characteristics, drought intensity differences caused by vegetation type, temperature, elevation, manmade irrigation, and other factors under the same water condition must be considered (Kallis, 2008; Zhang et al., 2009). The integration of traditional meteorological data, remotely sensed drought indices, together with information on elevation, vegetation type, and man-made irrigation, provides a promising approach to better characterize the spatial extent and intensity of drought. This research method becomes an urgent problem for further drought investigation.

The Classification And Regression Tree (CART) confers unique advantages in establishing a drought index compared with the traditional statistical regression techniques. It can handle a variety of data types (e.g. nominal, interval, and ratio data), and data without a normal distribution (non-parametric) and hierarchical relationships among variables (Brown et al., 2008). CART can also process large data volumes efficiently and has transparent, interpretable model outputs (De'ath and Fabricius, 2000). Tadesse et al. (2005) first proved the effectiveness of data-mining methods in drought risk management, identification, and monitoring. Using the regression tree model, the Vegetation Drought Response Index (VegDRI) was established (Brown et al., 2008). VegDRI uses PDSI as the dependent variable and incorporates different types of independent variables, including meteorological indices, remotely sensed indices, and biophysical data. Presently, this method has been used for near-real time drought monitoring throughout the United States. However, the VegDRI is still in a stage of improvement, and it needs further refinement. For example, the VegDRI mainly utilizes drought indices calculated from precipitation and vegetation conditions to detect the spatial extent and intensity of drought without other environmental variables, such as land surface temperature. The characteristics of drought indices and methods of optimal inputs selection for an integrated drought index need to be investigated in future research (VegDRI, 2011).

The objective of this paper is to establish a new integrated drought monitoring method named Integrated Surface Drought Index (ISDI) based on the concept of VegDRI. By selecting the best combination of variables with better accuracy, this method integrates the land surface water and thermal environment conditions, vegetation growth conditions, and biophysical information. This paper uses the ISDI to derive drought-detected results by considering the spatial extent and intensity of drought in mid-eastern China from 2000 to 2009. The results of the ISDI are then evaluated in terms of the spatial and temporal aspects to verify the advantage of the newly integrated drought monitoring model with respect to the accuracy, spatial resolution, and the application potential for drought identification in China.

2. Study area and data

2.1. Study area

Mid-eastern China was chosen as the study area (Fig. 1), covering 16% of the whole country (31–44.5°N, 109–123°E). This area includes 11 provinces and is mainly located in the semi-arid and arid area that span middle latitudes and in the semi-humid and semi-arid area of the warm temperate zone (Zheng and Li, 2008). Historically, severe droughts have frequently occurred in mid-eastern China because of the uneven spatial distribution of precipitation caused by the East Asian monsoon climate. The study area incorporates complex terrain, including the North China Plain and the mountains, the whole Shandong hilly area, the western part of Liaohe Plain and the eastern part of the Inner Mongolia Plateau.

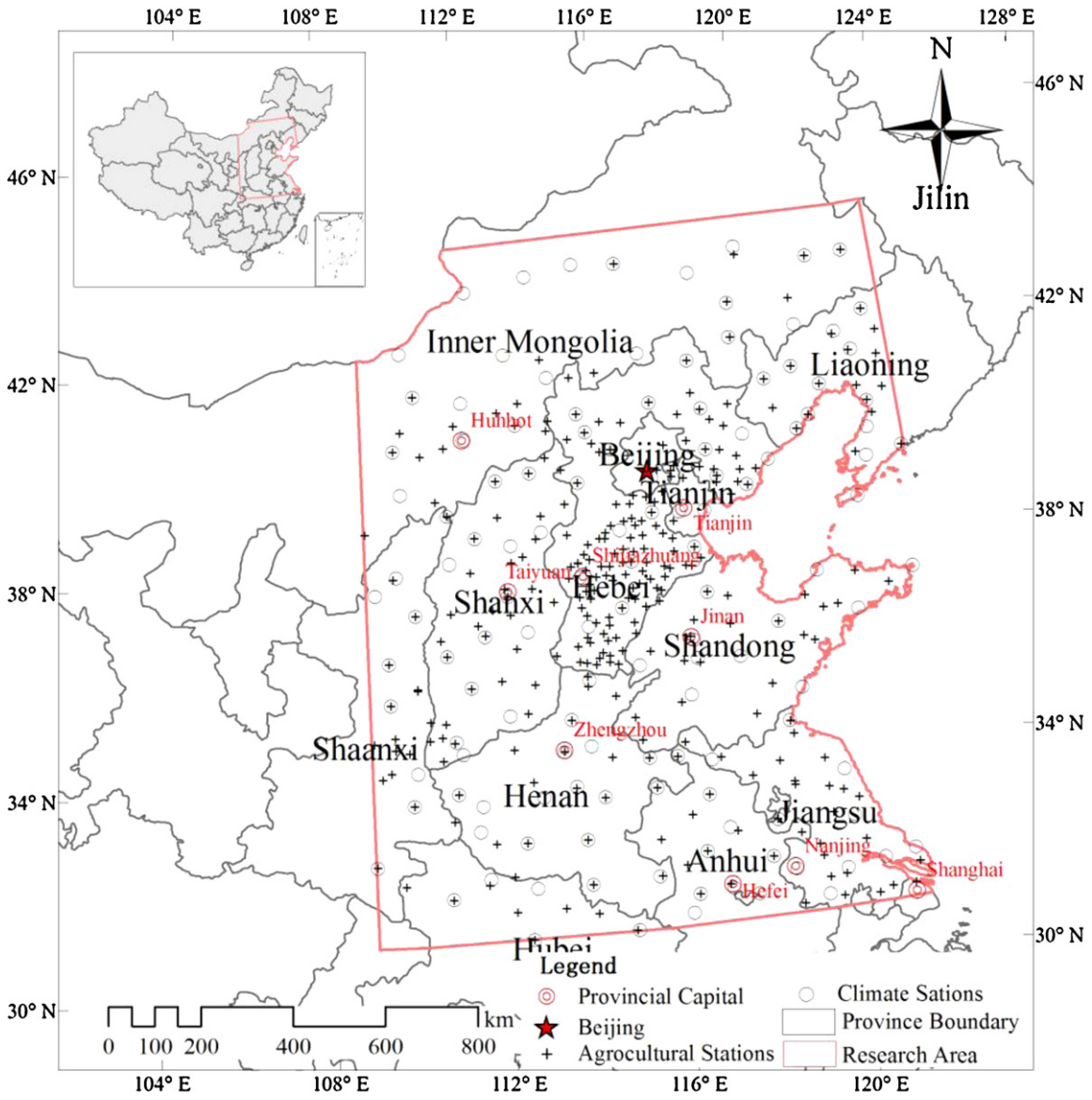

Fig. 1. Study area and the distribution of meteorological stations/agro-meteorological stations.

The land-cover type of this area is also rich with crops, grassland and deciduous broad-leaf forest. The ISDI was originally designed to integrate multiple data sources and affords good comparability in various regions. The ability of the ISDI in drought monitoring can be adequately evaluated in this study area. If the ISDI has the capability for drought monitoring in this area, the potential for a nationwide application of the ISDI can be identified, and the use of the ISDI can be extended to other parts of the world.

2.2. Data

Data used in this research includes the in situ meteorological data, agro-meteorological disasters dataset, remotely sensed data, and biophysical data. The meteorological data was acquired from the China Meteorological Data Sharing Service System (http://cdc.cma.gov.cn/). Data of daily precipitation and temperature during 50 years (1960–2009) from 130 weather stations in the study area was selected as the data source. The agro-meteorological disaster 10-day interval observation dataset (2000–2009) of 298 agro-meteorological sites in the study area was also obtained from the China Meteorological Data Sharing Service System. The 16-day Maximum Value Composited (MVC) MODIS NDVI time series products (MOD13A2, 1 km × 1 km) from 2000 to 2009, an 8-day average value of composited Land Surface Temperature (LST) products (MOD11A2, 1 km × 1 km) from 2000 to 2009 and the land cover data (MOD12Q1, 500 m × 500 m) for 2007 of the study area were acquired from U.S. National Aeronautics and Space Administration (NASA) Land Processes Distributed Active Archive Center (LP DAAC). The LST 8-day products were composited to 16-day products by calculating the average value of adjacent images to maintain the same temporal resolution as that of the NDVI dataset. The ecological zoning data was derived from a Chinese eco-geographical zoning map (Zheng and Li, 2008) and converted into a 1 km resolution raster image. Available water-holding capacity (AWC) data was extracted from global 10 km resolution Profile Available Water Capacity (PAWC) data provided by the International Geosphere-Biosphere Programme (IGBP). The irrigation water management distribution data was obtained from the Global Irrigation Area Map (GIAM, 10 km-8 classes: Version 2.0) released by the International Water Management Institute (IWMI) with a 10 km resolution. The Digital Elevation Data (DEM) was derived from the "China Western Environment and Ecology Science Data

Center" (http://westdc.westgis.ac.cn) with a spatial resolution of 1 km. The AWC, and irrigation zoning data were interpolated from 10 km into a 1 km raster image (Land cover data was interpolated from 500 m to 1 km) using the Kriging Interpolation method provided by ArcGIS 9.3 software to ensure a consistent spatial resolution. The Kriging method is an advanced geostatistical procedure that generates an estimated surface from scattered set of points with attribute values. It is proved to be a useful statistical downscaling method for the earth's surface biophysical properties (Voltz and Webster, 1990).

3. Methodology

3.1. Remotely sensed data and meteorological data processing

3.1.1. Remote sensed data processing

The Terra MODIS LST and NDVI products were processed to remove cloud-contaminated pixels using the quality control documents before used as inputs to calculate drought indices. The NDVI data sets are 16-day MVC products. However, there are still noise in the NDVI time series caused by cloud contamination and atmospheric variability, which greatly affects the accuracy of the vegetation dynamics (phenology) measurements and drought indices. In this paper, a simple, but robust, method based on the Savitzky–Golay filter (Savitzky and Golay, 1964) was used to reduce the noise and to construct a high-quality NDVI time-series (Chen et al., 2004). This approach has advantages in smoothing out noises and reflecting the genuine variation pattern of NDVI iteration process. We applied this method to the NDVI time-series for mid-eastern China during the 10-year period from 2000 to 2009.

3.1.2. Meteorological data processing

The daily rainfall data and temperature data were rigorously examined before importing them as data sources to calculate the meteorological drought indices (PDSI and SPI). The missing measurements were replaced by linearly interpolated values at the corresponding period of the adjacent two-years. The trace precipitation value, which cannot be recorded, was defined as 0.01 mm. Daily meteorological data was converted into a 16-day dataset. An accumulation method was used to process the rainfall data, but the average temperature value was calculated for a span of 16 days.

3.2. Data inputs for the integrated model

To fully describe the drought characteristics, various drought indices and land surface biophysical data were selected to characterize the vegetation growth condition, vegetation water stress, surface water and thermal environments, and regional drought differences (Table 1).

3.2.1. Climate data inputs for ISDI

In this study, the 16-day interval self-calibrated PDSI and multi-scale SPI (1-month, 2-month, 3-month, 6-month, 9-month, and 12-month) during 1960–2009 based on observed meteorological data were calculated using the processed meteorological data. The AWC input values for PDSI calculation are the average values extracted using the central 9 km × 9 km window at the site location based on the AWC raster map.

3.2.2. Satellite data inputs

Remotely sensed drought index inputs, i.e. VCI, TCI, VSWI, PASG, and Start of Season Anomaly (SOSA) (Table 2) were calculated based on the 16-day MODIS NDVI products and averaged 16-day LST. The VCI, PASG and SOSA within the six drought indices were created to detect drought condition through monitoring vegetation growth condition and vegetation phenophase anomalies based on the NDVI time series data. TCI is used to monitor drought through the land surface anomalies based on thermal infrared remote sensing information. The VSWI approach, which is an additive combination of NDVI and thermal data, was calculated to detect vegetation stress, moisture, as well as drought affected areas (Zhou et al., 2012).

In order to calculate the PASG, the Seasonal Greenness (SG) metric for each 16-day period was calculated for the 10 years time series. SG was obtained using the accumulated NDVI above the base line across the 16 days using the NDVI interpolated between the smoothed high-quality NDVI in consecutive 16-day composites (Zhou et al., 2012). The computing method is shown as Eq. (1):

$$SG = \int_{P1} (NDVI - NDVI_b) + \int_{P1} (NDVI - NDVI_b) + \cdots + \int_{P16} (NDVI - NDVI_b) \quad (1)$$

where $P1, P2, \ldots, P16$ refer to the day in a 16-day period. NDVI is the linearly interpolated smoothed value in the MODIS composited data and $NDVI_b$ is the latent NDVI value defined at the start of the growing season. PASG was then generated using equation in Table 2.

SOSA was calculated at the pixel level for each year as the equation in Table 2. Crop phenology was represented using a series of piecewise logistic functions of time using processed time-series NDVI products (Zhou et al., 2010). The onset and end of greenness were identified by the rate of change in the curvature of the fitted logistic models (Zhang et al., 2003).

3.2.3. Biophysical data

In this study, the biophysical inputs of ISDI include the Land Cover Data, Ecological Zoning Data, Irrigation Water Management Distribution Data, AWC, and DEM. The Land Cover data was included in the ISDI to reflect the different drought characteristics exhibited by each land cover type. The Ecological Zoning Data was selected to reflect the different environmental characteristics (for example, growing season length and plant species) across the study area. The Irrigation Water Management Distribution Data exhibits the great difference of vegetation sensitivity to drought caused by the irrigation. AWC represents the potential of the soil to hold moisture and make it available to plants. DEM accounts for the basic climate conditions and the solar energy budget difference.

3.2.4. Combination plans of the variables

The determination of the combination of variables is challenging because each drought index tends to focus on one aspect of drought characteristics, and the drought monitoring capacity of drought indices varies at different stages of the vegetation growing season across different regions. In our research, 12 candidate combinations of drought indices and biophysical parameters were designed to establish the integrated drought index.

First, the common variables in each combination were ascertained, including the SOSA, SPI, land cover, AWC, GIAM, and eco-geographical region. The SOSA index provides a measure of how the start of the growing season for a special year compares to the historically average level for the same period. The SPI can be used to quantitatively reflect the water deficit status of the select period compared to the historical average precipitation. Other biophysical variables were used to reflect the regional differences of drought.

Second, the appropriate inputs were selected to reflect the vegetation growth condition (or water stress), land surface temperature or the integrated inputs that can reflect both vegetation growth condition and land surface temperature at the same time. The available inputs included NDVI, PASG, VCI, LST, TCI, and VSWI. With dependent variables and common independent variables kept constant, inputs mentioned above were added into the scheme

Table 1
Data inputs for the integrated drought monitoring model construction.

Name	Type	Acronym	Source	Format	References
Palmer Drought Severity Index	Climate	PDSI	China Meteorological Data Sharing Service System	At sites	Palmer (1965)
Standardized Precipitation Index	Climate	SPI	China Meteorological Data Sharing Service System	At sites	McKee et al. (1993)
Normalized Difference Vegetation Index	Satellite	NDVI	Land Processes Distributed Active Archive Center (LP DAAC)	1 km raster	http://lpdaac.usgs.gov/get_data
Land Surface Temperature	Satellite	LST	LP DAAC	1 km raster	http://lpdaac.usgs.gov/get_data
Vegetation Condition Index	Satellite	VCI	Calculated using NDVI	1 km raster	Kogan (1995, 1997)
Temperature Condition Index	Satellite	TCI	Calculated using LST	1 km raster	Kogan (1995, 1997)
Vegetation Supply Water Index	Satellite	VSWI	Calculated using NDVI and LST	1 km raster	Bayarjargal et al. (2006), McVicar and Bierwirth (2001)
Start of Season Anomaly	Satellite	SOSA	Calculated using NDVI	1 km raster	Brown et al. (2008)
Percent of Average Seasonal Greenness	Satellite	PASG	Calculated using NDVI	1 km raster	Brown et al. (2008)
Elevation	Biophysical	DEM	Environmental & Ecological Science Data Center for West China, National Natural Science Foundation of China	1 km raster	http://westdc.westgis.ac.cn
Ecological Regions	Biophysical	EcoRe	China's Eco_Geographical Region Map	Vector	Zheng and Li (2008)
Land Cover	Biophysical	LanCo	LP DAAC	500 m raster	http://lpdaac.usgs.gov/get_data
Soil Available Water Capacity	Biophysical	AWC	International Geosphere-Biosphere Programme (IGBP)	10 km raster	http://www.igbp.net/
Irrigated Agriculture Region	Biophysical	IrrAg	Global Map of Irrigated Area (GIAM)	10 km raster	http://www.fao.org/nr/water/

to construct the integrated index. The accuracy was compared among the integrated indices, including the one obtained solely with the vegetation information or the temperature information and the one integrating VSWI, which contains information on both vegetation and temperature. Six Combinations of this type each contains a total of seven independent variables.

Third, we selected the elevation data as an additional input for four out of six combinations mentioned above, which showed higher regression accuracy. In this step, four combinations each consist of eight independent variables. We used this method to test if the elevation data can further improve the accuracy of the models.

Finally, groups of two indices PASG, TCI or VCI, TCI were used to characterize information on the vegetation condition and surface temperature anomalies. Elevation information was included in the scheme as well. The differences in precision of combinations were compared while building the comprehensive model. Each of the two combinations of this type contains a total of nine independent variables.

3.3. Integrated multisource data mining technology

A commercial CART algorithm (Cubist 2.07) was used in this investigation to analyze the historical drought indices and biophysical variables and to build the three seasonal, rule-based, linear regression models (Quinlan, 1993, 1996). The methodological flowchart of the integrated drought model is shown in Fig. 2.

Table 2
Computing method of data inputs for ISDI based on satellite data.

Drought indices	Formula	Source and reference
(1) Vegetation Condition Index (VCI)	$VCI_{ijk} = \frac{NDVI_{ijk} - NDVI_{i,\min}}{NDVI_{i,\max} - NDVI_{i,\min}}$	Kogan (1995, 1997)
(2) Percent of Average Seasonal Greenness (PASG)	$PASG_{i,PnYn} = (SG_{i,PnYn}/xSG_{i,Pn}) \times 100$ $SG = \int_{P1=SOS}^{Pn=EOS} NDVI$	Brown et al. (2008)
(3) Temperature Condition Index (TCI)	$LST_{ijk} = \frac{LST_{i,\max} - LST_{ijk}}{LST_{i,\max} - LST_{i,\min}}$	Kogan (1995, 1997), Bayarjargal et al. (2006)
(4) Vegetation Supply Water Index (VSWI)	$VSWI_{ijk} = NDVI_{ijk}/LST_{ijk}$	McVicar and Bierwirth (2001)
(5) Start of Season Anomaly (SOSA)	$SOSA_i = SOST_i - SOST_{med}$	Brown et al. (2008)

$NDVI_{ijk}$ – 16 day MVC NDVI for pixel i in period j for year k.
$NDVI_{i,\min}$ and $NDVI_{i,\max}$ – Multiyear minimum and maximum NDVI, respectively, for pixel i.
$SG_{i,PnYn}$ – SG for pixel i in period Pn for year Yn.
$xSG_{i,Pn}$ – Multiyear average SG(x) for pixel i in period Pn.
$P1$, Pn – The median start and end of the growing season (SOST, EOST).
LST_{ijk} – Land surface temperature for pixel i in period j for year k.
$LST_{i,\min}$ and $LST_{i,\max}$ – Multiyear minimum and maximum LST, respectively, for pixel i.
$SOSA_i$ – SOSA (in number of the days) for year i.
$SOST_i$ – Start of season DOY for year i.
$SOST_{med}$ – Median start of season DOY from 2000 to 2009.

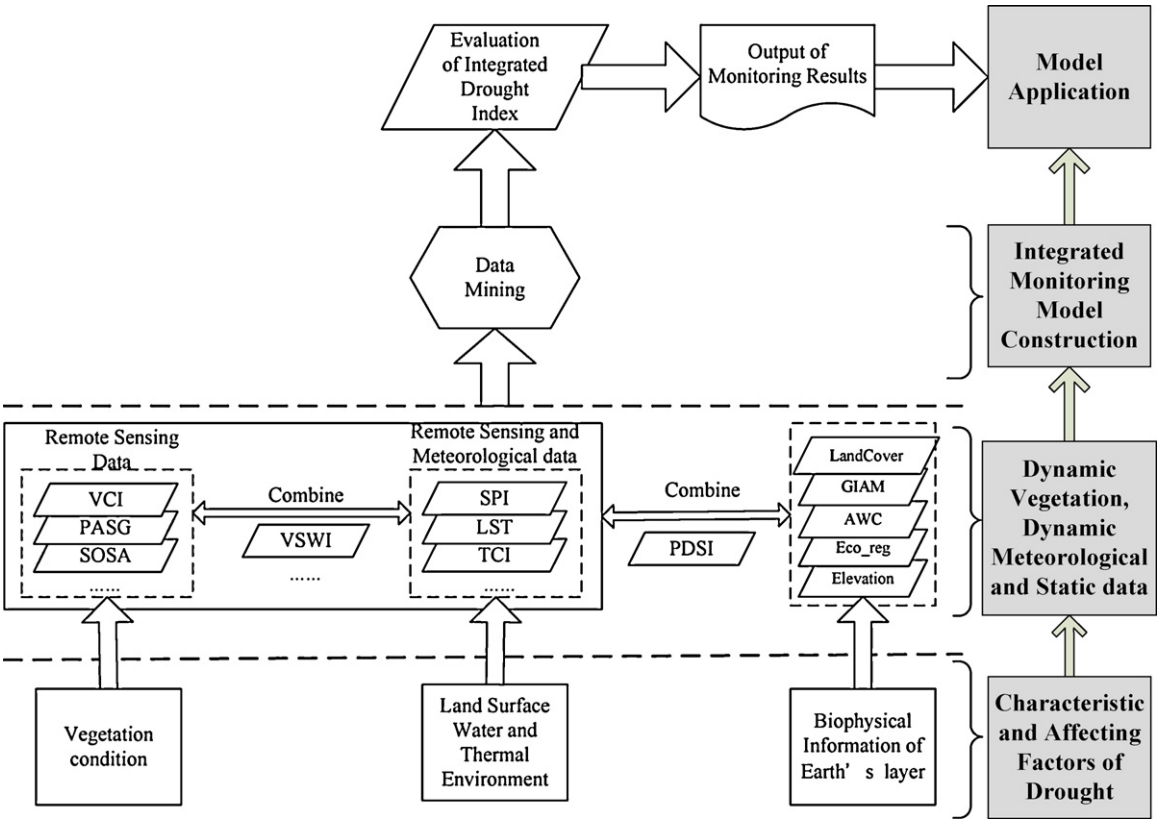

Fig. 2. Methodological flow-chart of the Integrated Surface Drought Index (ISDI).

The core idea of CART model is divided into two categories: classification and regression. First, by comparing the information gain of all the properties, the test attribute with the maximum value is selected as the classification criterion to construct the first-grade decision tree. The same method is used for the cycling treatment and stepwise refinement. The multilevel decision tree is constructed, and finally, the leaf nodes are generated. Then, a set of unordered rules are generated based on the statistical regression of the classified variables.

3.4. The integrated model construction method

The historical SPI and self-calibrated PDSI data for 130 meteorological stations in the study area were collected. The PDSI was selected as the dependent variable in the ISDI model for three primary reasons. First, unlike other meteorological drought indices, the PDSI not only combines the precipitation and temperature information but also factors the regional differences in Soil Available Water Content. Second, the PDSI value offers advantages in identifying multiple levels of drought severity and better comparability in different regions. Third, the drought monitoring capability of the PDSI has been validated in many regions of the world, and it has been identified as the national standard for meteorological drought monitoring in China. Brown et al. (2008) revealed that the 52-week SPI is suitable for the spring and summer VegDRI model, and the 40-week SPI is suitable for the fall model. Thus, in this paper, the 12-month SPI was selected as the independent variable for the spring and summer phase of the ISDI models, and the 9-month SPI was used as the fall ISDI model.

For the remotely sensed drought indices, the information from the $9\,km \times 9\,km$ pixel window centered on each station location was extracted, and the average value from the window was calculated for this continuous variables to represent the value of the site location. The NDVI, LST, PASG, TCI, and VSWI were sequentially extracted for the same period as the SPI and PDSI. The SOSA has one value each year. The elevation, AWC, GIAM, and eco-region were considered to be the inherent properties of the Earth. There was little change in the land-cover types in the study area during the research period of 2000–2009, thus, land cover was also considered to be a constant variable. The $9\,km \times 9\,km$ pixel window method was also applied to land cover data but the dominant (or majority) class in each window was selected to represent the value of the site location. As the vegetation has different sensitivities to water stress during different growth stages (Wu et al., 2010), the growing season was divided into three seasonal phases: spring, summer and fall. The specific time-dividing method is shown in Table 3.

The training database of all the aforementioned variables was assembled for all the weather stations from 2000 to 2009. The database was temporally subdivided into three seasonal subdivisions corresponding to the three seasonal phases. Then, the three datasets were imported into the Cubist 2.07 software, and the instances and rules mode in the software were used to analyze the data. The outputs of Cubist are a series of unordered rules, with the syntax as the following example:

Table 3
Three seasonal modeling phases for the ISDI.

Phase	Start date (DOY)	End date (DOY)	Phenological stage
Spring	65	145	Growing season started, early growth
Summer	145	241	Maturity, Peak growth
Fall	241	337	Senescence, harvest

Table 4
Drought grades classification of ISDI.

Drought intensity	ISDI value
Wet	$1 < ISDI$
Normal	$-1 < ISDI \leq 1$
Mild drought	$-2 < ISDI \leq -1$
Moderate drought	$-3 < ISDI \leq -2$
Severe drought	$-4 < ISDI \leq -3$
Extreme drought	$ISDI \leq -4$

Rule:
If: SOSA > 10, SPI ≤ −0.59, Elevation ≤ 1461.9, AWC ≤ 260
Then: $ISDI = -0.4118 + 1.01 \times SPI - 0.009 \times SOSA - 0.0069 \times AWC$

The appropriate rules were applied to the raster format input data for each 16-day period. The site-scale SPI variable was interpolated to 1 km raster images using the Inverse Distance Weighting (IDW) method. If the variables associated with a pixel met the threshold criteria identified by one rule, then the multivariate linear regression equation associated with this rule was used to calculate the ISDI value. If a pixel met two or more rules, then the results of all the rules were averaged to calculate the final ISDI value. Finally, the ISDI monitored maps were obtained with 16-day intervals spanning the period 2000–2009 and the drought grades classification of ISDI is shown in Table 4.

3.5. Evaluation of ISDI drought monitoring behavior using in situ drought observations

Eleven representative ago-meteorological sites were selected to verify the spatial monitoring results of the ISDI under four principles: first, the spatial distribution of selected site is relatively uniform; second, the sites have a good observational basis, and the observed data are relatively complete; third, the sites can represent three main land-cover types (crops, grassland and forests); and fourth, these sites are located in irrigated or non-irrigated areas, while the elevation of the sites is also obviously different. The agro-meteorological disaster 10-day interval observation dataset is sorting-out in statistics of agro-meteorological 10-day or monthly reports from the agro-meteorological sites. The dataset includes observed disaster name, afflicted crops, disaster degree, disaster intensity, affected area, and afflicted percentage during the period from September 1991 until now. In this paper, the ISDI monitored drought-affected agriculture area ($ISDI < -1$) and afflicted percentage of the cunty (or city) area where the agro-meoteological sites located in was calculated. Then, the ISDI monitored results were compared with the agro-meteorological disaster 10-day interval observation datasets. This quantitative analysis can be used to illustrate the detailed spatial resolution and localized drought monitoring capabilities provided by ISDI. Although this evaluation was limited to 11 representative sites and in 2006 which is the typical dry year, drought conditions and patterns characterized by ISDI for

Table 5
Comparison of 12 contribution results of the integrated drought monitoring model.

No.	Independent variables	# of variables	Phase	Average error	Relative error	Correlation coefficient
1	PASG, SOSA, SPI, Landcover, AWC, GIAM, Eco_region	7	Spring	0.3688	0.24	0.94
			Summer	0.7152	0.42	0.87
			Fall	0.3984	0.2	0.95
2	VSWI, SOSA, SPI, Landcover, AWC, GIAM, Eco_region	7	Spring	0.4444	0.29	0.91
			Summer	0.8025	0.47	0.83
			Fall	0.5396	0.28	0.92
3	VCI, SOSA, SPI, Landcover, AWC, GIAM, Eco_region	7	Spring	0.5754	0.38	0.88
			Summer	0.9007	0.53	0.81
			Fall	0.5873	0.31	0.91
4	TCI, SOSA, SPI, Landcover, AWC, GIAM, Eco_region	7	Spring	0.651	0.43	0.85
			Summer	0.8894	0.52	0.82
			Fall	0.6044	0.32	0.90
5	LST, SOSA, SPI, Landcover, AWC, GIAM, Eco_region	7	Spring	0.5376	0.35	0.89
			Summer	0.8312	0.49	0.84
			Fall	0.5091	0.27	0.92
6	NDVI, SOSA, SPI, Landcover, AWC, GIAM, Eco_region	7	Spring	0.4605	0.3	0.91
			Summer	0.7621	0.45	0.85
			Fall	0.5733	0.3	0.91
7	**VSWI, SOSA, SPI, elevation, Landcover, AWC, GIAM, Eco_region**	**8**	**Spring**	**0.3569**	**0.23**	**0.94**
			Summer	**0.7064**	**0.42**	**0.87**
			Fall	**0.4105**	**0.22**	**0.95**
8	TCI, SOSA, SPI, elevation, Landcover, AWC, GIAM, Eco_region	8	Spring	0.5522	0.36	0.90
			Summer	0.7922	0.46	0.86
			Fall	0.4625	0.24	0.94
9	LST, SOSA, SPI, elevation, Landcover, AWC, GIAM, Eco_region	8	Spring	0.4467	0.29	0.92
			Summer	0.7257	0.43	0.87
			Fall	0.4078	0.21	0.95
10	NDVI, SOSA, SPI, elevation, Landcover, AWC, GIAM, Eco_region	8	Spring	0.3619	0.24	0.94
			Summer	0.6376	0.37	0.89
			Fall	0.4291	0.22	0.94
11	PASG, TCI, SOSA, SPI, elevation, Landcover, AWC, GIAM, Eco_region	9	Spring	0.5399	0.35	0.89
			Summer	0.7398	0.43	0.87
			Fall	0.4524	0.24	0.94
12	VCI, TCI, SOSA, SPI, elevation, Landcover, AWC, GIAM, Eco_region	9	Spring	0.6209	0.41	0.88
			Summer	0.7976	0.47	0.86
			Fall	0.5579	0.29	0.92

this area are fairly representative of the whole mid-eastern China area.

To further analyze the temporal drought monitoring behavior of ISDI during the whole study period, the ISDI 16-day interval monitoring results at the agro-meteorological sites from 2000 to 2009 were extracted using the 9 km × 9 km window. The ISDI average value of all pixels in the extraction window was calculated to represent the drought degree at the site location. At the same time, the corresponding drought and flood observational records during the same period were obtained from the agro-meteorological sites. The trend of the corresponding relationship between the ISDI monitored results and field observation results were compared. In comparing the ISDI monitored values and corresponding observations, the observation results were assigned according to the level of drought and flood conditions. The smaller values of the ISDI represent the more severe drought, while the greater values represent more abundant rainfall. 1, 2, 3, and 5 represent severe drought, moderate drought, mild drought, and continuous rain or flood condition, respectively. The capability of ISDI used for drought monitoring during different period can be evaluated using this method.

4. Results and discussion

4.1. Precision of the integrated model construction

The specific construction schemes of the integrated drought index are shown in Table 5.

The 12 schemes in Table 5 can be divided into 3 groups according to the number of independent variables in the model: schemes (1)–(6) with 7 independent variables, schemes (7)–(10) with 8 independent variables and schemes (11) and (12) with 9 independent variables. Comparison of the 3 groups of scheme shows that schemes (7)–(10) have the highest overall accuracy, with the correlation coefficient larger than 0.9 in spring and fall phases, and the correlation coefficients of summer are also larger than 0.86. The schemes (1)–(6) and schemes (11) and (12) have the similar accuracy, with the correlation coefficients in the range of 0.8–0.94. This indicates that the regression accuracy is not proportional to the number of independent variables when constructing the integrated drought monitoring model. The most high-precision schemes in Table 5 are schemes (7), (1), and (10). The overall accuracy of scheme (7) is slightly higher than scheme (1), with the lower average error of 0.3569 and 0.7064 in spring and summer phases respectively. Only the average error (0.4105) in fall phase of scheme (7) is a little larger than scheme (1). Scheme (10) only has higher accuracy in summer phase than scheme (7) and scheme (1), with correlation coefficient reaches 0.89, while the accuracy of spring and fall phase are both lower than the two schemes mentioned above, with average error of 0.3619 and 0.4291, respectively.

Many studies have demonstrated that the land surface temperature has a significant impact on the vegetation growth status (Wang et al., 2001a,b; Wang et al., 2003; Yang et al., 1997). High temperature has an important effect in terms of causing and aggravating drought (Yang et al., 1998). The integrated model containing VSWI and elevation (Table 5(7)) performs more precisely than the models with single information (Table 5(1)–(6), (8)–(10)) or the combinations of VCI, TCI and PASG, TCI (Table 5(11) and (12)). Through comparing all of the schemes, we found that scheme (7) is the most suitable scheme for calculating ISDI values. In addition to the best regression accuracy among schemes in Table 5 on average, scheme (7) which incorporated VSWI, elevation and other information, can comprehensively characterize drought in that it considered not only the vegetation condition but also the surface water content and thermal environment anomaly. Therefore, we choose scheme (7) to calculate the ISDI. The scatter plots of scheme (7) predictions and real values established using all sequences of historical variables as the training database are presented in Fig. 3.

4.2. ISDI regional monitoring capabilities for a typical dry year

The average SPI series of the meteorological stations in the study area indicated that the annual precipitation in 2006 was less than normal level (Zhou et al., 2012). The disaster observations (including drought, flood, gale, hail, diseases and insect pests) of agro-meteorological stations also demonstrated that many regions in this study area experienced various levels of drought at different times in 2006. Thus, 2006 was selected as a typical dry year to analyze the temporal and spatial effectiveness of the ISDI. The monitoring results of which at four typical periods (DOY 145, 161, 241, and 305) are provided in Fig. 4.

Linfen, Xilinhot, Taian, Xuchang, Shangzhou, and Boxian are among the 11 selected agro-meteorological stations in the study area with drought field observation data in 2006. The observed drought records are listed in Table 6.

The ISDI drought monitored results at the regional scales are consistent with the field observation records of the agro-meteorological stations. Fig. 4(a)–(d) indicates that the study area has experienced various levels of drought during May and November of 2006. The northern part of study area, including Inner Mongolia, Shanxi, northern Shaanxi, Hebei, and Liaoning provinces, experienced serious drought which lasted almost throughout the entire growing season of 2006, and the most serious drought occurred before June 2006; in particular, the drought intensity in central Mongolia, including the Xilinhot site, reached a severe level. According to the field observation records, the Xilinhot site in eastern Inner Mongolia experienced 4 months of drought from early May to early September of 2006. Approximately 90–100% of the region was impacted by drought. The Linfen station experienced 70 days of mild drought from April to June of 2006, and the damaged area reached approximately 30–49% of the entire region. These results have good consistency with the monitoring results of Fig. 4(a) and (b). The ISDI monitored results demonstrate that the southern parts of the study area, including Henan, Shandong, Jiangsu, Anhui, Hubei, and Southern Shannxi, received ample rainfall before June 2006 and some areas experienced partial water logging. Some local regions between Xuchang and Boxian at the eastern part of Henan province suffered severe drought. The field drought observations of the Xuchang and Boxian agro-meteorological sites indicate that severe drought occurred in this area during mid-April and early June (Table 6). Boxian experienced moderate drought, and the drought-impacted area covered 90–100% of the entire county. The ISDI monitored results demonstrate that the drought began to spread after August (Fig. 4c and d). Some areas of Shandong peninsula, Henan, southern Shannxi, and Hubei began to suffer drought, and the drought was aggravated after August. The drought center in the northern study area shifted to two sides, expanding from the middle part of Inner Mongolia to both the eastern and western parts. The drought was aggravated at the common border of Liaoning, Shaanxi, and Inner Mongolia provinces and the drought classification reached the extreme drought level, while the drought in northern Hebei province exhibited some mitigation. Corresponding to the ISDI drought monitoring results, the field observations at the Taian station indicate that Taian suffered persistent drought from late October to December of 2006, and the drought gradually became more serious during that period.

For evaluating the drought monitoring accuracy of the ISDI on a local scale with quantitative analysis, the drought-affected agriculture area (ISDI < −1) of the city area including Xilinhot, Linfen, Taian, and Shangzhou was counted at four typical periods. The

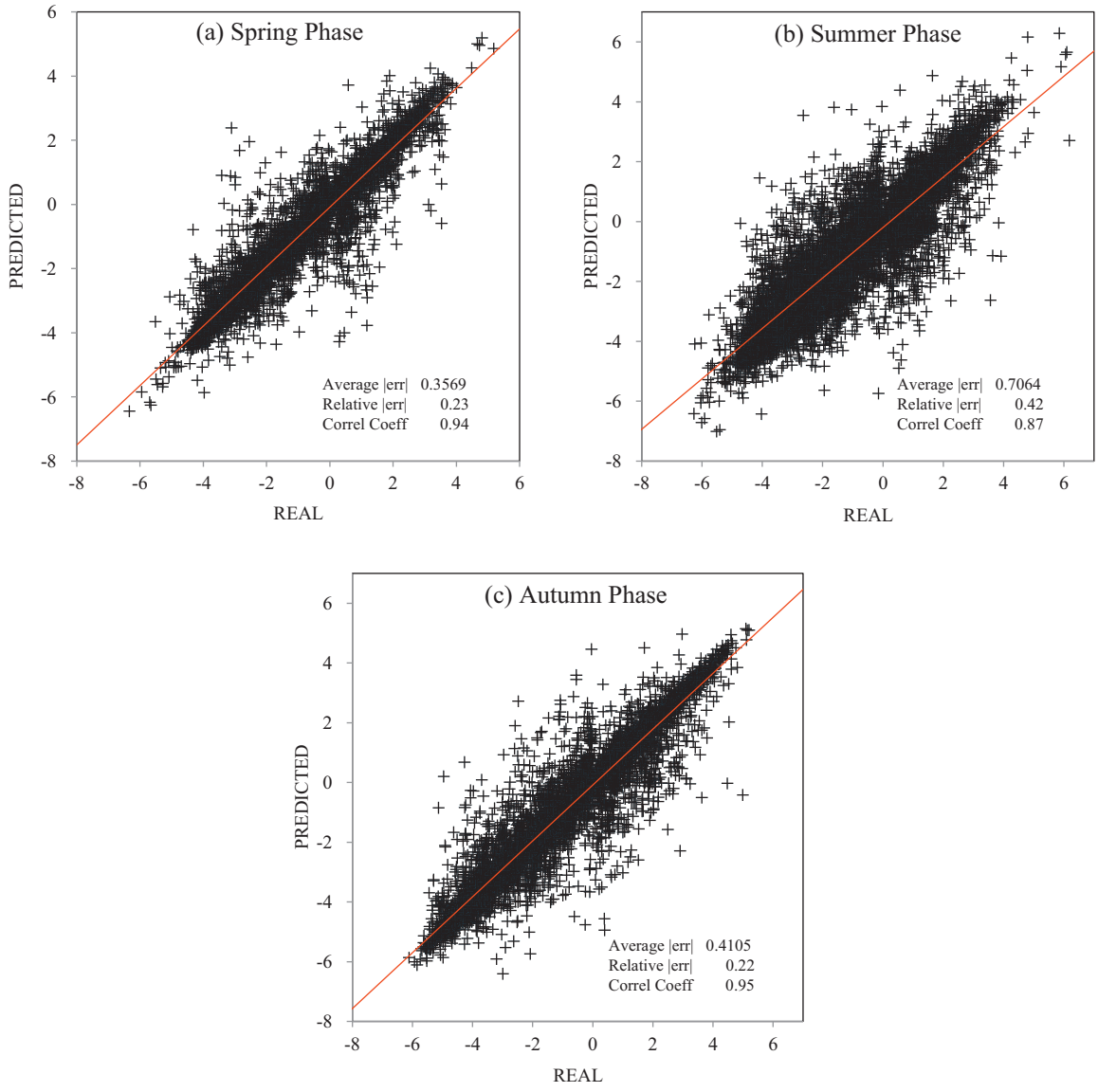

Fig. 3. Scatter plots for scheme 7 predicted values and real values. The real values are the PDSI time series calculated based on observed meteorological data at meteorological stations. The predicted values are the ISDI values calculated based on independent variables using the rules generated by Cubist 2.07. The 'Average |err|' represents the average of ISDI error of all samples. The 'Relative |err|' is the ratio of average error magnitude to the error magnitude that would result from always predicting the mean value. 'Correl Coeff' represents the correlation coefficient between PDSI and ISDI.

corresponding relationship between the monitored results and those of the estimated stricken area was compared. The results are shown in Table 7.

Table 7 shows that ISDI also offers good monitoring accuracy on the local scale. The percentage of drought-affected areas monitored by the ISDI is consistent with the percentage observed at agro-meteorological sites, and the overall errors are within 10%. In particular, the percentage of the observed drought-affected area of Xilinhot reaches 90–100% in late May, late June, and early September of 2006, while the ISDI monitored result is 95.83%

Table 6
Drought field observations of selected 6 agro-meteorological stations in the study area for 2006.

Site name	Longitude (°E)	Latitude (°N)	Drought occurrence time (2006)
Linfen	111.5	36.06	April
Linfen	111.5	36.06	May to early June
Xilinhot	116.12	43.95	Early May to early September
Taian	117.15	36.16	Late April to early May
Taian	117.15	36.16	Late October to early November
Taian	117.15	36.16	Mid-November to late November
Taian	117.15	36.16	December
Xuchang	113.85	34.01	Mid-April to early May
Shangzhou	109.96	33.86	In mid-June
Boxian	115.77	33.87	Late April to mid-June

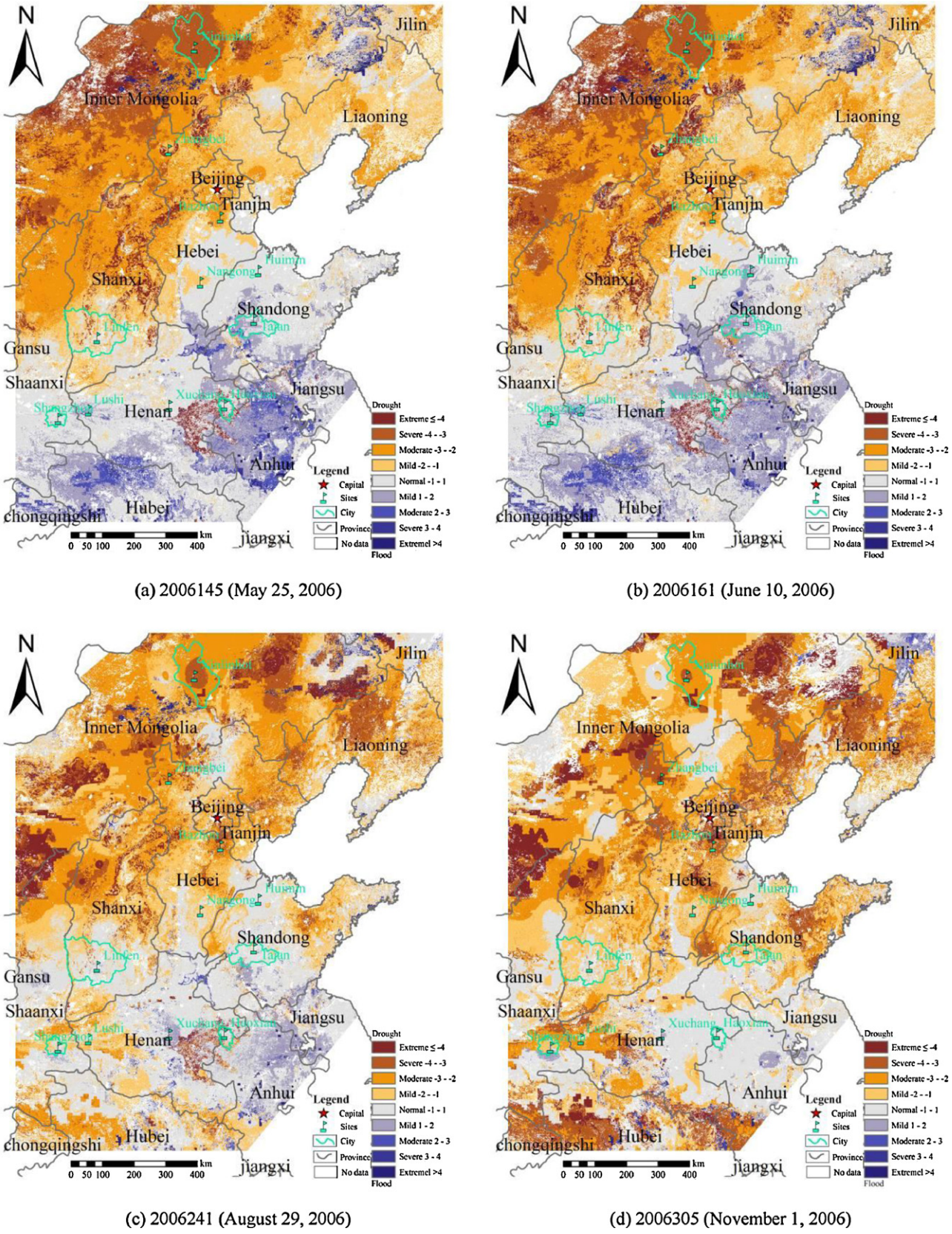

(a) 2006145 (May 25, 2006)

(b) 2006161 (June 10, 2006)

(c) 2006241 (August 29, 2006)

(d) 2006305 (November 1, 2006)

Fig. 4. ISDI drought monitored results in mid-eastern China for DOY 2006145 (May 25, 2006), and DOY 2006161 (June 10, 2006), DOY 2006241 (August 29, 2006), DOY 2006305 (November 1, 2006). The green line is the corresponding city or county range in which the selected agro-meteorological stations are located. (For interpretation of the references to color in this figure legend, the reader is referred to the web version of the article.)

Table 7
Comparison of the drought field observations and the ISDI monitored results in 2006.

Site name	Year	Month	Ten days	Intensity	Affected area (ha)	Observed percentage	Date (DOY)	ISDI monitored percentage
Xilinhot	2006	5	3	Mild	>66,666	90–100%	145	95.83%
Xilinhot	2006	6	3	Mild	>66,666	90–100%	161	95.83%
Xilinhot	2006	9	1	Mild	>66,666	90–100%	241	95.83%
Linfen	2006	6	1	Mild	13,333	40–49%	145	55.01%
Taian	2006	11	2	Mild	40,000	60–69%	305	50.02%
Shangzhou	2006	6	2	Mild	7333	10–19%	161	9.84%

Mild: dry soil layer appears and the dry-soil depth is less than 3 cm. The upper leaves of crop roll because of lack water.
Mid: The dry soil depth is 3–6 cm. The leaves of crop wilt during the day because of drought persistence.
Affected Area (ha) is crop area affected by drought.
Percentage is the ratio of drought affected crop area and sown area in the county where the agro-meteorological site located in. The values are estimated results through observation.

(Fig. 4a–c). The results of the two methods are very close in value. The percentage of the observed drought-affected area is between 40 and 49%, while the ISDI monitored result is 55.01% (ISDI < −1) (Fig. 4a). The error between the observed result and the monitored result is approximately 5%. Taian suffered persistent drought from late October to December. The percentage of the drought-affected area is between 60% and 69% in mid-November, while the ISDI monitored result is 50.02%. In addition, the afflicted percentage observation is in accordance with the ISDI result. The afflicted percentage results of the agro-meteorological sites are estimated through in situ observations. The main observations are the agricultural drought level and soil moisture. However, the ISDI combines many other drought characteristics and influencing factors, including the traditional precipitation data, remotely sensed vegetation conditions, and land surface water and thermal environment anomalies. The ISDI can comprehensively reflect the drought condition, and therefore, it exhibits some differences with the field observations in the expression of drought characteristics. Thus, the ISDI monitored results do not entirely correspond to the field observations. In addition, the estimated observation results are vulnerable to subjective human factors. Generally, the error is approximately 10%. The man-made differences in criteria among the different sites will also produce some errors. Thus, the 10% error between the ISDI monitored results and field observation results are in the normal range of error fluctuation. All of the agro-meteorological sites in Table 7 suffered mild drought, while the ISDI monitored results of Xilinhot clearly reached severe drought levels at DOYs 145 and 161 (Fig. 4a and b). The differences between the ISDI and observations are also due to the reasons listed above.

4.3. The relationship between agro-meteorological site observations and the ISDI-derived drought intensity

The corresponding changes in the relation between the ISDI monitoring results and site observations from 2000 to 2009 are shown in Fig. 5.

Fig. 5 shows that the overall change trend of the ISDI values and the trend of field observation results at the agro-meteorological stations are basically the same, which demonstrates that ISDI has good monitoring capabilities on local scale (same as or less than county areas). All of the ISDI series trends in Fig. 5 indicate that the value of the ISDI becomes smaller with a continuous drought or an increase in disaster levels. The ISDI monitoring results go up with the mitigation of the drought level and disaster reduction. The ISDI at the sites during the drought period shows a pattern similar to the trough of a wave, but also reaches a large value in non-dry periods. The ISDI value increase rapidly, even reaching a maximum during the flood period or with the continuous rainfall. All of the ISDI series from Taian, Shangzhou, and Boxian reflect the variation characteristics. This indicates that the ISDI can be used to accurately monitor the occurrence of droughts and floods. Zhangbei and Xilinhot, which are located in the northern study area, have less annual precipitation and surface water content than those of other sites. Correspondingly, the overall ISDI values are less than those at other sites. To a certain extent, the ISDI can reflect the general surface water content.

The ISDI values corresponding to three drought levels show some differences among different sites but range from −2 to 0. The ISDI values corresponding to moderate drought levels have a larger range of −4 to −1. The ISDI corresponding to severe drought levels has a range of −5 to −3, while the range corresponding to floods is 0–4. The ISDI values corresponding to three observed drought levels are not strictly distinct. This is because drought intensity derived from human observation is determined according to the crop growth conditions and soil moisture. The classifications of three drought levels are not perfectly defined because of the differences in drought criteria used by different people at different agro-meteorological stations. However, the ISDI has a comprehensively quantitative characterization of drought, combining traditional precipitation data and remotely sensed thermal and water content environment status conditions. The ISDI and observations exhibit some differences in the description of drought characteristics. In addition, ISDI can detect more detailed drought conditions with five levels of drought while the field observation at agro-meteorological sites only has three drought categories. This means that one observed drought value will necessarily correspond to a range of ISDI values, causing the difference between the corresponding ISDI value and observed results at different sites and different times.

5. Conclusions

This research comprehensively monitored drought characteristics in terms of vegetation growth condition, surface water and thermal environment, and biophysical information. The ISDI was established using data-mining technology, which uses the PDSI as a dependent variable and eight other factors as independent variables based on the traditional meteorological drought data, remotely sensed data, and biophysical data. Previous studies have demonstrated that the land surface temperature has a significant influence on drought, and it contributes more to the result of a hybrid index, such as VSWI, than the reflective signal (Zhou et al., 2010). By comparing the average error, relative error, and correlation coefficients of the 12 drought indices combinations, combination with VSWI involved, which considered temperature information and has high regression accuracy, is finally selected to calculate the ISDI.

The ISDI is suitable for large-scale (larger than provincial or national area) drought monitoring. ISDI can monitor the drought onset, extension, and evolution. The regional drought monitoring effectiveness of the ISDI has been validated during all periods of 2006 in mid-eastern China. Moreover, the ISDI also offers good

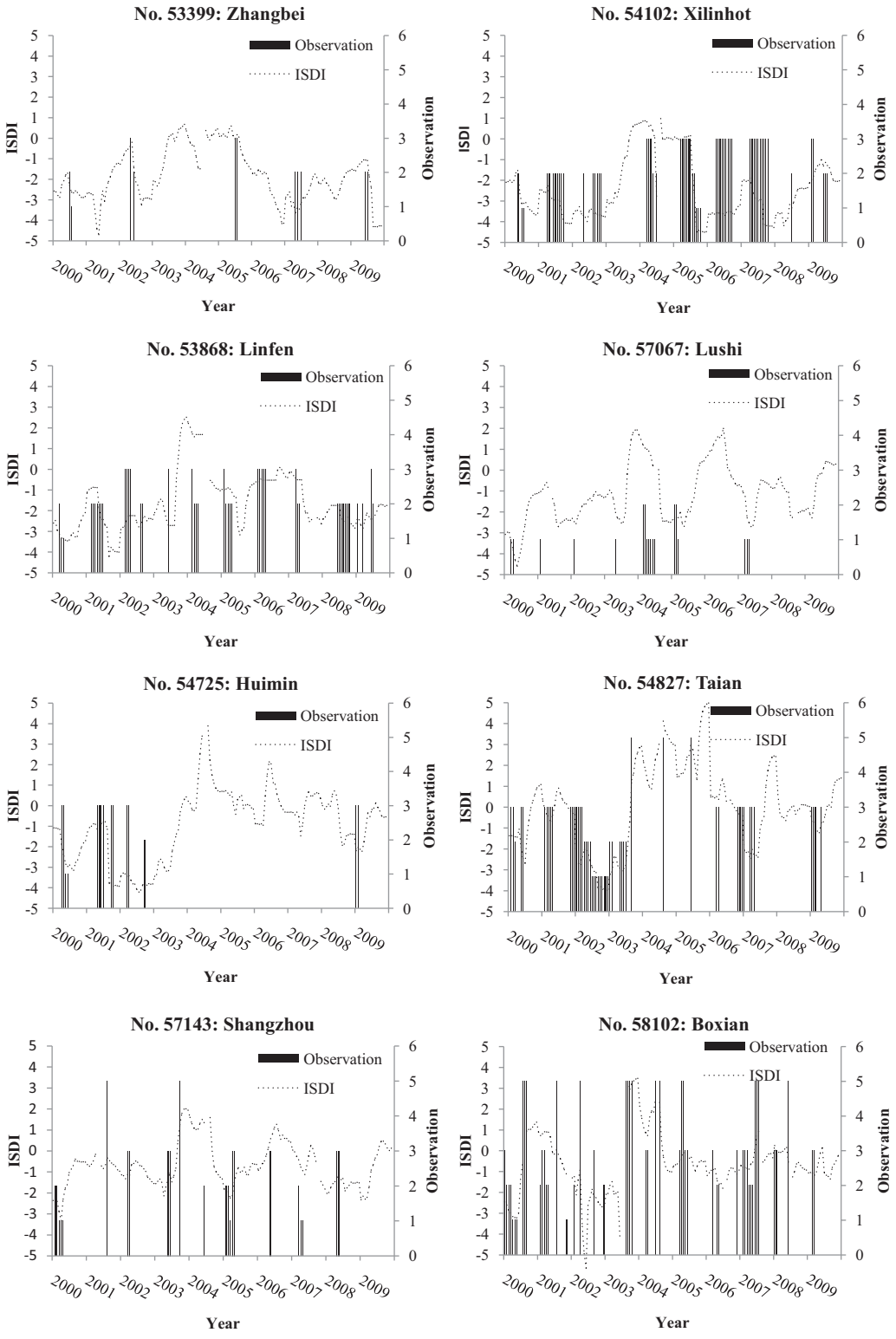

Fig. 5. Comparison of the site-scale ISDI monitored results and field observations from 2000 to 2009.

capability for monitoring spatial variations in drought condition on local scale (same as or less than county areas). The percentage of drought-affected areas monitored by the ISDI has good agreement with the percentage observed at the agro-meteorological sites. Though limited by the time interval of MODIS NDVI, the ISDI monitoring results have a 16-day interval that can be implemented in a near-real-time fashion to monitor the spatial and temporal changes of a drought. Future research will focus on shortening the time interval of the ISDI results to provide operational and timely information to users.

Using the multi-year disaster data set observed at the agro-meteorological sites, the capability and effectiveness of the ISDI were analyzed at the site scale across 2000–2009. The results indicate that ISDI can be used to accurately monitor the occurrence of

drought and it can characterize detailed drought categories. ISDI has the capability to reflect both the amount of precipitation and the severity of drought caused by lack of rainfall. The multi-year, multi-region quantitative field observation data (e.g. soil moisture and crop yield) collected at agro-meteorological sites will be used to further determine the precision and performance of this index.

Acknowledgments

This work was funded by the National Natural Science Foundation of China through the project 'Investigation of Regional Agricultural Drought Monitoring Approach Based on Simulation of Crop Growth Process (41171403)' and the CRSRI Open Research Program (CKWV2012320/KY). The authors would like to thank Ruijing Jia for her helpful editorial support and the reviewers of the manuscript for their helpful comments. We are also grateful to Dr. Aifeng Lü, Bin He, Lin Zhao, and Xinyu Mo for their useful suggestions.

References

Alley, W.M., 1984. The Palmer Drought Severity Index: limitations and assumptions. Journal of Applied Meteorology 27 (7), 1100–1109.
Bannari, A., Morin, D., Bonn, F., Huete, A.R., 1995. A review of vegetation indices. Remote Sensing Reviews 13 (1), 95–120.
Bayarjargal, Y., et al., 2006. A comparative study of NOAA-AVHRR derived drought indices using change vector analysis. Remote Sensing of Environment 105 (1), 9–22.
Berliner, P., Oosterhuis, D.M., Green, G.C., 1984. Evaluation of the infrared thermometer as a crop stress detector. Agricultural and Forest Meteorology 31 (3/4), 219–230.
Boken, V.K., Cracknell, A.P., Heathcote, R.L., 2005. Monitoring and Predicting Agricultural Drought: A Global Study. Oxford University Press, Oxford, UK, pp. 3–8.
Brown, J., Wardlow, B., Tadesse, T., Hayes, M., Reed, B., 2008. The Vegetation Drought Response Index (VegDRI): a new integrated approach for monitoring drought stress in vegetation. GIScience Remote Sensing 45 (1), 16–46.
Chen, J., et al., 2004. A simple method for reconstructing a high-quality NDVI time-series data set based on the Savitzky-Golay filter. Remote Sensing of Environment 91 (3-4), 332–344.
Chen, J., Wang, B., Gao, X., 2012. Scale correction of two-band ratio of red to near-infrared using imagery histogram approach: a case study on Indian remote sensing satellite in Yellow River Estuary. IEEE Journal of Selected Topics in Applied Earth Observation 5 (2), 663–668.
Dai, A., Trenberth, K.E., 1998. Global variations in droughts and wet spells: 1900–1995. Geophysical Research Letters 25 (17), 3367–3370.
Dracup, J.A., Lee, K.S., E.G.P. Jr., 1980. On the definition of droughts. Water Resources Research 16 (2), 297–302.
De'ath, G., Fabricius, K.E., 2000. Classification and regression trees: a powerful yet simple technique for ecological data analysis. Ecology 81 (11), 3178–3192.
Gibbs, W.J., 1975. Drought – its definition, delineation and effects. World Meteorological Organization, Geneva, Switzerland.
Gillies, R.R., Carlson, T.N., 1995. Thermal remote sensing of surface soil water content with partial vegetation cover for incorporation into climate models. Journal of Applied Meteorology 34 (4), 745–756.
Gillies, R.R., Kustas, W.P., Humes, K.S., 1997. A verification of the 'triangle' method for obtaining surface soil water content and energy fluxes from remote measurements of the Normalized Difference Vegetation Index (NDVI) and surface radiant temperature. International Journal of Remote Sensing 18 (15), 3145–3166.
Gutman, G.G., 1990. Towards monitoring droughts from space. Journal of Climate 3 (2), 282–295.
Guttman, N.B., 1997. Comparing the Palmer Drought Index and the Standardized Precipitation Index. Journal of American Water Resource Association 34 (1), 113–121.
Guttman, N.B., 1999. Accepting the standardized precipitation index: a calculation algorithm. Journal of American Water Resource Association 35 (2), 311–322.
Henricksen, B.L., Durkin, J.W., 1986. Growing period and drought early warning in Africa using satellite data. International Journal of Remote Sensing 7 (11), 1583–1608.
Jackson, R.D., Idso, S.B., Reginato, R.J., 1981. Canopy temperature as a crop water stress indicator. Water Resources Research 17 (4), 1133–1138.
Justice, C.O., Townshend, J.R.G., Holben, B.N., Tucker, C.J., 1985. Analysis of the phenology of global vegetation using meteorological satellite data. International Journal of Remote Sensing 6 (8), 1271–1318.
Kallis, G., 2008. Droughts. Annual Review of Environment and Resources 33 (1), 85–118.
Kogan, F.N., 1990. Remote sensing of weather impacts on vegetation in non-homogeneous areas. International Journal of Remote Sensing 11 (8), 1405–1419.
Kogan, F.N., 1995. Droughts of the late 1980 in the United States as derived from NOAA polar-orbiting satellite data. Bulletin of American Meteorological Society 76 (5), 655–668.
Kogan, F.N., 1997. Global drought watch from space. Bulletin of American Meteorological Society 78 (4), 621–636.
Li, K., Guo, Q., Zhang, J., 1999. China Drought Research and Disaster mitigation measures. Henan Science and Technology Press, Zhengzhou, China (in Chinese).
Liu, W.T., Kogan, F.N., 1996. Monitoring regional drought using the Vegetation Condition Index. International Journal of Remote Sensing 17 (14), 2761–2782.
Ma, Z., Dan, L., Hu, Y., 2004. The extreme dry/wet events in northern China during recent 100 years. Journal of Geographical Science 14 (3), 275–281.
McKee, T.B., Doesken, N.J., Kleist, J., 1993. The relationship of drought frequency and duration to time scales. In: Eighth Conference on Applied Climatology, Meteorological Society, Anaheim, CA, USA, pp. 179–184.
McVicar, T.R., Bierwirth, P.N., 2001. Rapidly assessing the 1997 drought in Papua New Guinea using composite AVHRR imagery. International Journal of Remote Sensing 22 (11), 2109–2128.
McVicar, T.R., Jupp, D.L.B., 1998. The current and potential operational uses of remote sensing to aid decisions on drought exceptional circumstances in Australia: a review. Agricultural Systems 57 (3), 399–468.
Misshra, A.K., Singh, V.P., 2010. A review of drought concepts. Journal of Hydrology 391, 202–216.
Mottram, R., DeJager, J.M., Duckworth, J.R., 1983. Evaluation of a water stress index for maize production using an infra-red thermometer. Crop Protection 12, 26–28.
Palmer, W.C., 1965. Meteorological drought. U.S. Weather Bureau Research Paper 45, 58.
Pinter, P.J., et al., 1979. Remote detection of biological stresses in plants with infrared thermometry. Science 205 (4406), 585–587.
Price, J.C., 1990. Using spatial context in satellite data to infer regional scale evapotranspiration. IEEE Transactions on Geoscience and Remote Sensing 28, 940–948.
Quinlan, J.R., 1993. C4.5 Programs for Machine Learning. Morgan Kaufmann Publishers, San Francisco, CA, USA.
Quinlan, J.R., 1996. Improved use of continuous attributes in C4.5. JAIR 4, 77–90.
Rasmussen, M.S., 1998. Developing simple, operational, consistent NDVI-vegetation models by applying environmental and climatic information. Part I: Assessment of net primary production. International Journal of Remote Sensing 19 (1), 97–117.
Savitzky, A., Golay, M.J.E., 1964. Smoothing and differentiation of data by simplified least squares procedures. Analytical Chemistry 36 (8), 1627–1639.
Son, N.T., Chen, C.F., Chen, C.R., Chang, L.Y., Minh, V.Q., 2012. Monitoring agricultural drought in the Lower Mekong Basin using MODIS NDVI and land surface temperature data. International Journal of Applied Earth Observation and Geoinformation 18, 417–427.
Tadesse, T., Brown, J.F., Hayes, M.J., 2005. A new approach for predicting drought-related vegetation stress: Integrating satellite, climate, and biophysical data over the U.S. central plains. ISPRS Journal of Photogrammetry and Remote Sensing 59 (4), 244–253.
Tannehill, I.R., 1947. Drought, Its Causes and Effects. Princeton University Press, Princeton, NJ, USA.
Tucker, C.J., Choudhury, B.J., 1987. Satellite remote sensing of drought conditions. Remote Sensing of Environment 23 (2), 243–251.
Tucker, C.J., Sellers, P.J., 1986. Satellite remote sensing of primary production. International Journal of Remote Sensing 7 (11), 1395–1416.
Tucker, C.J., 1989. Comparing SMMR and AVHRR data for drought monitoring. International Journal of Remote Sensing 10 (10), 1663–1672.
VegDRI, 2011. VegDRI Frequently Asked Questions. http://www.drought.unl.edu/vegdri/VegDRI_faq.htm
Voltz, M., Webster, R., 1990. A comparison of kriging, cubic splines and classification for predicting soil properties from sample information. Journal of Soil Science 41 (3), 473–490.
Wan, Z., Dozier, J., 1996. A generalized split-window algorithm for retrieving land-surface temperature from space. IEEE Transactions on Geoscience and Remote Sensing 34 (4), 892–905.
Wan, Z., Wang, P., Li, X., 2004. Using MODIS Land Surface Temperature and Normalized Difference Vegetation Index products for monitoring drought in the southern Great Plain, USA. International Journal of Remote Sensing 25 (1), 61–72.
Wang, J., Price, K.P., Rich, P.M., 2001a. Spatial patterns of NDVI in response to precipitation and temperature in the central Great Plains. International Journal of Remote Sensing 22 (18), 3827–3844.
Wang, J., Rich, P.M., Price, K.P., 2003. Temporal responses of NDVI to precipitation and temperature in the central Great Plains, USA. International Journal of Remote Sensing 24 (11), 2345–2364.
Wang, P., Gong, J., Li, X., 2001b. Vegetation-Temperature Condition Index and its application for drought monitoring. Journal of Wuhan University (Information Science) 26 (5), 412–417.
Wilhite, D.A., Glantz, M.H., 1985. Understanding the drought phenomenon: the role of definitions. Water International 10 (3), 111–120.
Wilhite, D.A., 2000. Drought as a natrural hazard: concepts and definitions. In: Wilhite, D.A. (Ed.), Drought: A Global Assessment. Routledge, London & New York, pp. 3–8.
Wilhite, D.A., 2002. Preparing for drought: a methodology. In: Wilhite, D.A. (Ed.), Drought: a Global Assessment. Routledge, New York, USA, pp. 89–104.
Wilhite, D.A., Easterling, W.E., Wood, D.A., 1987. Planning for Drought: Toward a Reduction of Societal Vulnerability Understanding: the Drought Phenomenon: The Role of Definitions. Westview Press, Boulder, USA.
WMO, 1975. Drought and Agriculture. World Meteorological Organization, Geneva, Switzerland.

Wu, J., et al., 2010. Analysis of relationships among vegetation condition indices and Multiple-time Scale SPI of grassland in growing season. In: The 18th International Conference on Geoinformatics, Beijing, China, pp. 1–6.
Yang, L., Wylie, B.K., Tieszen, L.L., Reed, B.C., 1998. An analysis of relationships among climate forcing and time-Integrated NDVI of grasslands over the U.S. northern and central great plains. Remote Sensing of Environment 65 (1), 25–37.
Yang, W., Yang, L., Merchant, J.W., 1997. An assessment of AVHRR/NDVI-ecoclimatological relations in Nebraska, U.S.A. International Journal of Remote Sensing 18 (10), 2161–2180.
Zhang, Q., Pan, X., Ma, Z., 2009. Droughts. China Meteorological, Beijing, China (in Chinese).
Zhang, X., et al., 2003. Monitoring vegetation phenology using MODIS. Remote Sensing of Environment 84 (3), 471–475.
Zheng, D., Li, B., 2008. Study on Eco-geographic Regional Systems of China. The Commercial Press, Beijing, China (in Chinese).
Zhou, L., et al., 2010. Assessing the drought monitoring characteristic of time-series NDVI indices in crop growing season. In: IEEE International Geoscience and Remote Sensing Symposium, Honolulu, Hawaii, USA, pp. 2063–2066.
Zhou, L., et al., 2012. Comparison of remote sensed and meteorological data derived drought indices in mid-eastern China. International Journal of Remote Sensing 33 (6), 1755–1779.